TOPOLOGICAL MATTER

Bismuthene on a SiC substrate: A candidate for a high-temperature quantum spin Hall material

F. Reis,[1]* G. Li,[2,3]* L. Dudy,[1] M. Bauernfeind,[1] S. Glass,[1] W. Hanke,[3] R. Thomale,[3] J. Schäfer,[1]† R. Claessen[1]

Quantum spin Hall materials hold the promise of revolutionary devices with dissipationless spin currents but have required cryogenic temperatures owing to small energy gaps. Here we show theoretically that a room-temperature regime with a large energy gap may be achievable within a paradigm that exploits the atomic spin-orbit coupling. The concept is based on a substrate-supported monolayer of a high–atomic number element and is experimentally realized as a bismuth honeycomb lattice on top of the insulating silicon carbide substrate SiC(0001). Using scanning tunneling spectroscopy, we detect a gap of ~0.8 electron volt and conductive edge states consistent with theory. Our combined theoretical and experimental results demonstrate a concept for a quantum spin Hall wide-gap scenario, where the chemical potential resides in the global system gap, ensuring robust edge conductance.

Quantum spin Hall (QSH) systems are two-dimensional (2D) representatives of the family of topological insulators, which exhibit conduction channels at their edges that are inherently protected against certain types of scattering. Initially predicted for graphene (*1*, *2*) and eventually realized in HgTe quantum wells (*3*, *4*), in the QSH systems realized so far (*5*, *6*), the decisive bottleneck preventing applications is the small bulk energy gap of less than 30 meV. The chemical potential must reside safely within this gap to avoid detrimental contributions to the edge current from the bulk material, and very low temperatures (below that of liquid helium) are needed to suppress thermal excitation of charge carriers into those bulk electron bands (*7*, *8*). Strategies to shift the thermal operation limit above room temperature must, therefore, tailor the energy gap of the system toward substantially larger values.

Although the QSH phase is characterized by universal topological properties (*2*), other aspects such as the bulk energy gap are material specific and depend on the combination of spin-orbit coupling (SOC) (scaling as Z^4 in elements of atomic number Z), orbital hybridization, and the symmetries of the layer-substrate system. The minute SOC in graphene precludes a noticeable gap; one strategy to generate enhanced gaps in related QSH honeycomb-layer materials (*1*) is to use elements heavier than C. For systems with the group IV elements Si, Ge, and Sn, predicted gaps are 2 (*9*), 24 (*9*), and 100 meV (*10*), respectively. According to the Kane-Mele model (*1*), these gaps are still relatively small because SOC enters the gap determination only in higher-order perturbation theory. This applies to hypothetical freestanding materials with poor chemical stability. Real-world variants require a supporting substrate for epitaxial synthesis, which brings concurrent bonding interactions into play. Attempts were made to grow, for example, silicene on a metallic Ag substrate (*11*, *12*); however, this short-circuits any edge states of interest. An insulating MoS_2 substrate can stabilize germanene (*13*), yet the compressive strain renders the material a metal. Stanene flakes on Bi_2Te_3 are plagued by the same problem (*14*).

Turning to group V of the periodic table, bismuth (Z = 83) must be expected to yield an even larger gap. Its thin free-standing layers have been predicted to be topologically nontrivial (*15*–*17*). The existence of a monolayer bismuthene QSH phase on a silicon substrate has been proposed (*18*) and extended to a SiC substrate (*19*). However, experimental growth of a hexagonal single-layer Bi phase on Si(111) has failed (*20*, *21*).

Here we show, combining theory and experiment, that for bismuthene grown on a SiC(0001) substrate, the substrate is not only stabilizing the quasi-2D topological insulator but also playing a pivotal role for achieving the large gap, with the strong on-site SOC coming directly into play.

Our experimental realization of supported bismuthene uses a SiC(0001) substrate, on which we generate a $(\sqrt{3} \times \sqrt{3})$R30° superstructure of Bi atoms in honeycomb geometry (Fig. 1A and fig. S1). The resulting lattice constant of 5.35 Å is considerably larger than that of buckled Bi(111) bilayers. This causes a fully planar configuration of the honeycomb layer, which is energetically favorable (*19*). The synthesis described in (*22*) starts from a hydrogen-etched SiC wafer on which a monolayer of Bi is epitaxially deposited, giving rise to sharp electron diffraction peaks (fig. S2). A scanning tunneling microscopy (STM) overview (Fig. 1B) shows that the whole surface is smoothly covered with flakes of typical diameter ~25 nm, separated by phase-slip domain boundaries (related to the Bi-induced surface reconstruction), and includes occasional defects. Alternatively,

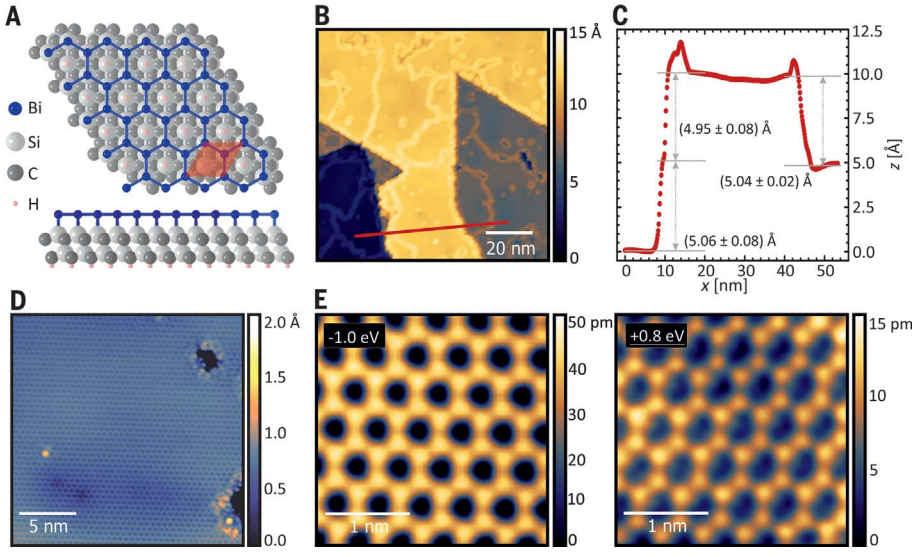

Fig. 1. Bismuthene on SiC(0001) structural model. (**A**) Sketch of a bismuthene layer placed on the threefold-symmetric SiC(0001) substrate in $(\sqrt{3} \times \sqrt{3})$R30° commensurate registry. (**B**) Topographic STM overview map showing that bismuthene fully covers the substrate. The flakes are of ~25-nm extent, limited by domain boundaries. (**C**) Substrate step-height profile, taken along the red line in (B). The step heights correspond to SiC steps. (**D**) The honeycomb pattern is seen on smaller scan frames. (**E**) Close-up STM images for occupied and empty states (left and right panels, respectively). They confirm the formation of Bi honeycombs.

[1]Physikalisches Institut and Röntgen Research Center for Complex Material Systems, Universität Würzburg, D-97074 Würzburg, Germany. [2]School of Physical Science and Technology, ShanghaiTech University, Shanghai 201210, China. [3]Institut für Theoretische Physik und Astrophysik, Universität Würzburg, D-97074 Würzburg, Germany.
*These authors contributed equally to this work. †Corresponding author. Email: joerg.schaefer@physik.uni-wuerzburg.de

the flakes are also terminated by steps of the SiC substrate (Fig. 1C). Inspection of the layer on a smaller scale reveals the characteristic honeycomb pattern of bismuthene (Fig. 1D). Detailed view of the honeycomb structure is provided by the STM close-up in Fig. 1E. For both occupied and empty states, the images show a honeycomb pattern throughout.

To establish that the electronic structure of the synthesized material corresponds to bismuthene, we performed angle-resolved photoelectron spectroscopy (ARPES) and compared the results with density-functional theory (DFT) (Fig. 2 and fig. S4). The electron bands in Fig. 2A are obtained by using a hybrid exchange-correlation functional, including SOC (*22*). At the K point, the direct energy gap amounts to 1.06 eV [six orders of magnitude larger than in graphene with ~1 μeV (*23*)]. The conduction-band minimum at Γ leads to an indirect gap of 0.67 eV in DFT. The momentum-resolved dispersion from ARPES in Fig. 2B exhibits the characteristic maximum at the K point and a band splitting there, in close agreement with the DFT overlay. From the ARPES close-up in Fig. 2C of the valence-band maximum at K, we derive a large band splitting of ~0.43 eV, subsequently identified as the distinct "Rashba fingerprint" of the system. The constant energy maps in Fig. 2D reflect the energy degeneracy of the K and K′ points and provide further proof of the high degree of long-range order in the Bi honeycomb lattice. The excellent agreement of ARPES and DFT results suggests the realization of a single bismuthene layer on SiC (while clearly excluding a double layer, see fig. S5).

Next, we disentangle the key mechanisms that determine the energetics near the Fermi level E_F by reducing (downfolding) the full DFT band structure to the relevant low-energy model [see (*22*) for details]. Inclusion of substrate bonding proves indispensable in this procedure. We decompose the band structure into σ-bond contributions formed by Bi 6s, p_x, and p_y orbitals and π-bond contributions formed by p_z orbitals. As a consequence of hybridization with the substrate via π bonds, the orbital content at low energies is predominantly of σ type (Fig. 3A), and p_x and p_y orbitals play the main role close to E_F, whereas the p_z orbital is pushed out of this energy region.

Focusing on the low-energy bands around the Fermi level, we find that, without relativistic effects, the mere orbital hybridization in the σ-bonding sector (with eight bands coming from twofold orbital, spin, and sublattice degrees of freedom) yields a Dirac-like band crossing at the K point (Fig. 3B). SOC affects the band structure through two leading contributions: First, the local (on-site) SOC term $\lambda_{SOC}L_z\sigma_z$ generates large matrix elements between p_x and p_y orbitals [see, e.g., (*24*)] and directly determines the magnitude of the energy gap at the K point (Fig. 3C), which is of order ~$2\lambda_{SOC}$. Second, the π-bonding sector hybridizes with the substrate, which breaks inversion symmetry. It features a Rashba term that, in leading order of perturbation theory, couples into the σ-bonding sector, yielding a composite effective Hamiltonian

$$H_{\mathrm{eff}}^{\sigma\sigma} = H_0^{\sigma\sigma} + \lambda_{SOC}H_{SOC}^{\sigma\sigma} + \lambda_R H_R^{\sigma\sigma}$$

where $H_0^{\sigma\sigma}$, $H_{SOC}^{\sigma\sigma}$, and $H_R^{\sigma\sigma}$ are specified in (*22*).

We derive the prefactors for Bi/SiC as λ_{SOC} ~ 0.435 eV and λ_R ~ 0.032 eV (*22*). Although the Rashba term λ_R is much smaller than λ_{SOC}, it induces the large valence-band splitting (as seen clearly in ARPES) into states of opposite spin character, while leaving the conduction band spin-degenerate at K (Fig. 3D). The six valence-band maxima are energy degenerate. Their large momentum separation and the huge Rashba splitting prevent spin scattering in the bulk (*25*), as discussed for 2D semiconductors.

The mechanism at work here produces a QSH phase with the nontrivial topological invariant $Z_2 = 1$ [see (*22*) and fig. S6 for derivation] and is very different from the Kane-Mele mechanism (*1*) for graphene. Graphene's gap emerges owing to SOC between next-nearest neighbors and at the level of second-order perturbation theory and is therefore minute. In other group IV monolayers, such as silicene, the SOC remains of the next-nearest–neighbor type (*26*), and the relevant orbital is still p_z. By contrast, in bismuthene, the low-energy physics is driven by the huge on-site SOC of p_x and p_y orbitals. This is also distinct from HgTe/CdTe quantum wells, where the small band gap is governed by a complex band situation and opens only upon strain (*3*, *4*).

Another fundamental ingredient that stabilizes the wide-gap QSH phase in bismuthene is the comparatively large lattice constant defined by the SiC-substrate registry. It corresponds to a planar configuration close to its energy minimum (*19*), i.e., is effectively strain-free and not subject to buckling. As argued for functionalized stanene (*10*), the topological gap is lost when external strain shifts another band through the gap. This phase transition to a trivial system is promoted by compressive strain, whereas tensile strain stabilizes the QSH phase. Not surprisingly, compressed germanene (*13*)

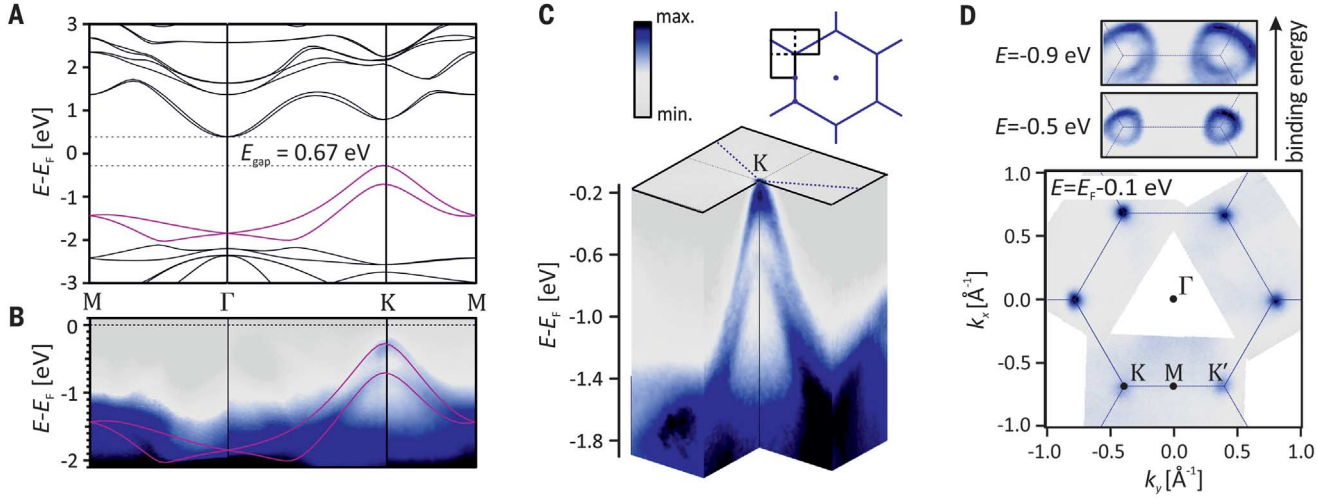

Fig. 2. Theoretical band structure and ARPES measurements. (**A**) DFT band-structure calculation (with a hybrid exchange-correlation functional) including SOC, showing the wide band gap and a substantial band splitting in the valence band (dashed line). For position of the critical points Γ, K, and M, see the surface Brillouin zone (SBZ) in (D). (**B**) ARPES band dispersion through the Brillouin zone. The band maximum at K and the valence-band splitting are in close agreement with the theoretical prediction (overlay). The zero of energy (E_F) is aligned to the Fermi level of the spectrometer. (**C**) Close-up of ARPES showing a valence-band maximum at the K point with large SOC-induced splitting in a wide momentum range. The sketch in the top-right corner depicts the orientation of the cut (black lines) in the momentum space of the SBZ (blue hexagon). (**D**) Constant-energy surfaces from ARPES at various binding energies. The cut at low binding energies is taken at the topmost intensity corresponding to the valence-band maximum. The maps are consistent with the sixfold degeneracy of the K and K′ points of the hexagonal lattice.

and stanene (*14*) have been reported to be metals, which highlights the importance of the substrate.

A landmark feature of QSH systems are the helical edge channels, connecting valence and conduction states by two bands of opposite spin (fig. S8), irrespective of the edge architecture (zigzag or armchair). Within the bulk gap, they exhibit an approximately constant density of states (DOS). In a ribbon simulation, the states rapidly decay toward the bulk within one unit cell, i.e., ~5 Å (fig. S8).

By using scanning tunneling spectroscopy (STS), the local DOS (LDOS) is inspected at the atomic scale. Bismuthene edges exist at SiC-substrate steps. Differential tunneling conductivity (dI/dV) curves, reflecting the LDOS, have been recorded along a path toward an uphill step in Fig. 4A (I, tunneling current; V, bias voltage). Far from the edge, the spectrum evidences a large bulk gap of ~0.8 eV. Notably, the tunneling spectrum reproduces both the Rashba fingerprint in the occupied states and the structure in the empty states (fig. S7). Closer to the boundary, a state emerges, filling the entire gap—as in the DFT ribbon model for both armchair and zigzag edges (fig. S8). Its signal increases continuously toward the edge, while retaining its shape and exhibiting

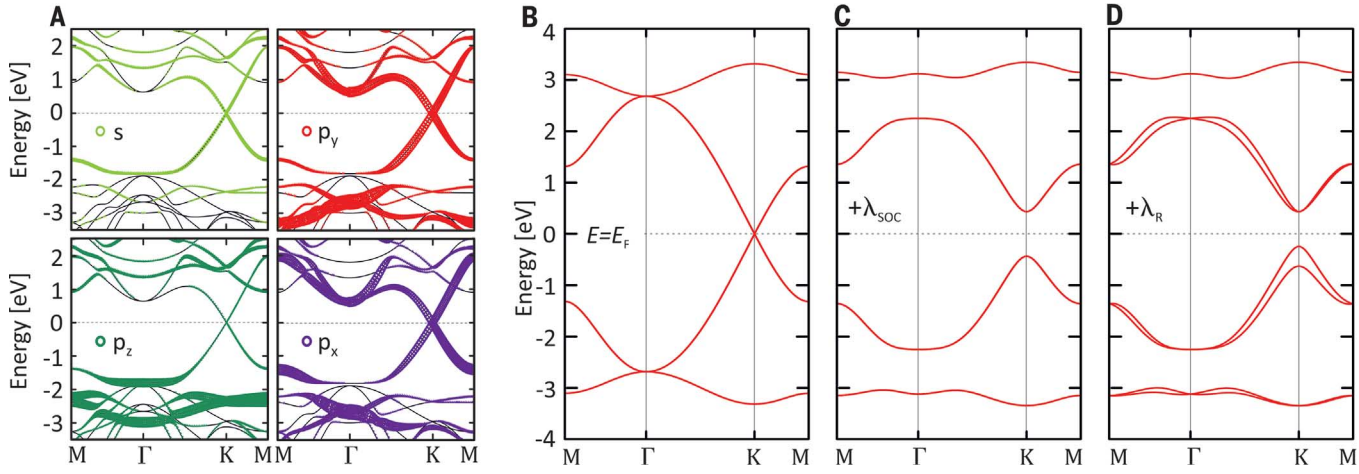

Fig. 3. Calculated electronic structure of the low-energy effective model of Bi σ bands. (**A**) The contribution of Bi s and p orbitals to the electronic structure of bismuthene (without SOC). In each panel, the symbol size is proportional to the relative weight of the orbital. In Bi/SiC, p_x and p_y orbitals prevail around E_F, demonstrating orbital decomposition. (**B**) Electronic structure of the low-energy effective model without SOC. (**C**) Inclusion of the strong atomic SOC opens a huge gap at the K point. (**D**) Further including the Rashba term lifts the degeneracy of the topmost valence band and induces a large splitting with opposite spin character there.

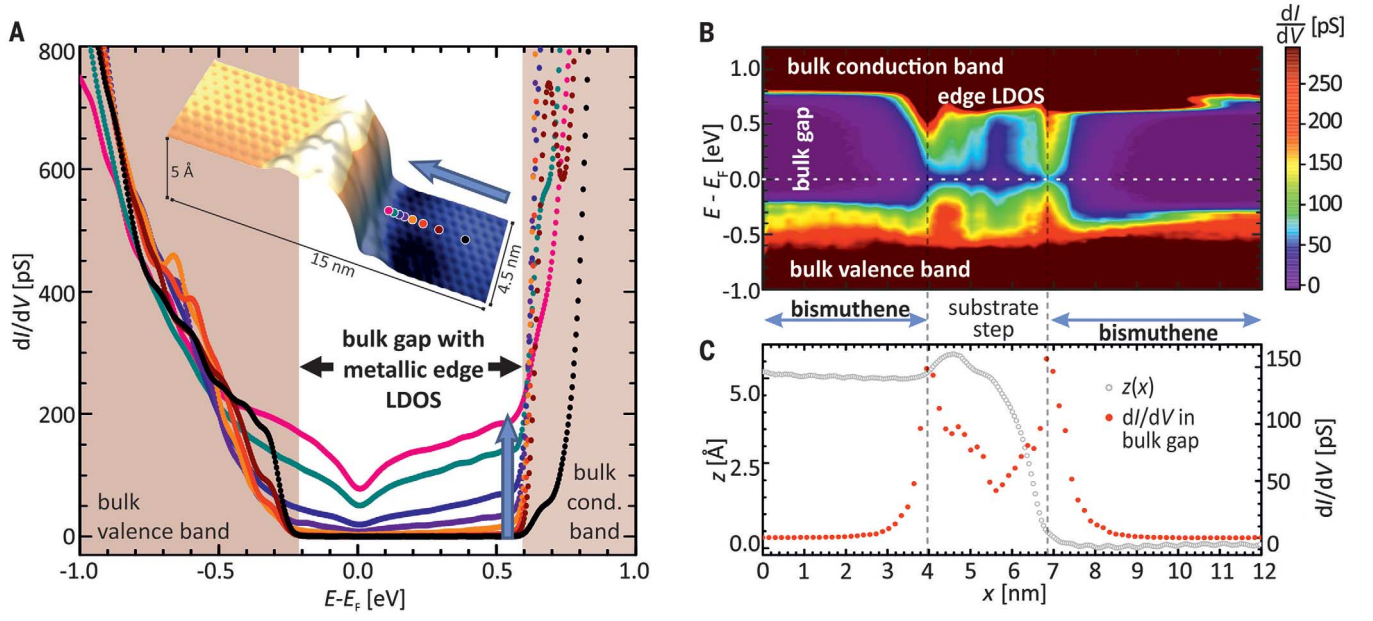

Fig. 4. Tunneling spectroscopy of edge states at substrate steps. (**A**) Differential conductivity dI/dV (reflecting the LDOS) at different distances to the edge. A large gap of ~0.8 eV is observed in bulk bismuthene (black curve). Upon approaching the edge, additional signal of increasing strength emerges that fills the entire gap. Inset: STS measurement locations (color-coded dots relate to spectrum color) at uphill substrate step causing the boundary. (**B**) Spatially resolved dI/dV data across the same step. The dI/dV signal of the in-gap states peaks at both film edges (gray dashed lines mark dI/dV maxima). (**C**) Topographic $z(x)$ line profile of the step and dI/dV signal of bismuthene (integrated over the gap from +0.15 to +0.55 eV), showing an exponential decrease away from the step edge, on either side.

a zero-bias anomaly, where dI/dV is suppressed. The anomaly may reflect tip-related electron scattering (*27*) or hint at Luttinger-liquid behavior of the edge channel (*28*), which requires further study. Indeed, this spectral dip is not an inherent property of the band structure–derived metallic DOS in the gap but is rather a many-body feature imprinted on top of it. This is evidenced by the dip remaining fixed to the chemical potential, irrespective of occasional small shifts of the bulk band edges (see, e.g., Fig. 4B and fig. S9). The edge DOS in Fig. 4B (see also figs. S9 and S10) shows equivalent behavior for upper and lower terrace, demonstrating the robustness against the particular geometric situation. The dI/dV signal (integrated over the gap) in Fig. 4C shows a decay length of (4 ± 1) Å, matching well with DFT for simple ribbon edges (fig. S8).

In this material system, it is the covalent bonding between the orbitals of the Bi monolayer with the substrate that generates the large topological gap, as well as giving rise to the stabilization of the compound system. This is in contrast to earlier theory work on hypothetical free-standing material (*15*, *17*, *29*), which cannot be used for applications. In experiments with bulk (metallic) Bi crystals, peeled-off layers reportedly show QSH conductance quantization (*30*), and in spectroscopy, topological states have been claimed at terrace steps (*31*). Edge states for a single Bi layer on Bi_2Te_3 of ~2-nm extent have been detected (*32*) within a small gap of ~70 meV, but with E_F in the substrate valence band. By contrast, in our case, E_F resides within both the bismuthene gap (~0.8 eV) as well as the SiC gap (3.2 eV), so that conduction should solely be governed by the edge states.

Although the topological character of the edge states has experimentally yet to be established, e.g., by a direct transport measurement of the QSH effect with its universal quantized conductance, the agreement between experimental evidence and theoretical prediction already strongly suggests that the QSH scenario in Bi/SiC is valid. For HgTe (*4*, *5*), the gap is ~30 meV, and in InAs/GaSb/AlSb quantum wells (*6*), it is ~4 meV, which necessitates experiments below 300 mK. The key problem in these systems is the "charge puddles," where defects push E_F into the bulk bands, overriding the 1D channel (*7*, *8*). By contrast, the large gap in bismuthene suggests that it may be operational at room temperature. The domain size of ~25 nm is expected to be increased by optimized epitaxial growth, facilitating transport measurements on patterned samples.

Our work demonstrates the decisive role of the substrate for controlling the relevant orbitals in 2D QSH insulators. Here, this approach is utilized to exploit the atomic (on-site) SOC to directly determine the topological energy gap. This kind of material engineering generates a paradigm in that it opens a systematic route to create large-gap QSH systems in monolayer-substrate composites, e.g., by using other group V elements.

REFERENCES AND NOTES

1. C. L. Kane, E. J. Mele, *Phys. Rev. Lett.* **95**, 226801 (2005).
2. C. L. Kane, E. J. Mele, *Phys. Rev. Lett.* **95**, 146802 (2005).
3. B. A. Bernevig, T. L. Hughes, S.-C. Zhang, *Science* **314**, 1757–1761 (2006).
4. M. König *et al.*, *Science* **318**, 766–770 (2007).
5. A. Roth *et al.*, *Science* **325**, 294–297 (2009).
6. I. Knez, R.-R. Du, G. Sullivan, *Phys. Rev. Lett.* **107**, 136603 (2011).
7. M. König *et al.*, *Phys. Rev. X* **3**, 021003 (2013).
8. J. I. Väyrynen, M. Goldstein, L. I. Glazman, *Phys. Rev. Lett.* **110**, 216402 (2013).
9. C.-C. Liu, W. Feng, Y. Yao, *Phys. Rev. Lett.* **107**, 076802 (2011).
10. Y. Xu *et al.*, *Phys. Rev. Lett.* **111**, 136804 (2013).
11. B. Lalmi *et al.*, *Appl. Phys. Lett.* **97**, 223109 (2010).
12. P. Vogt *et al.*, *Phys. Rev. Lett.* **108**, 155501 (2012).
13. L. Zhang *et al.*, *Phys. Rev. Lett.* **116**, 256804 (2016).
14. F.-F. Zhu *et al.*, *Nat. Mater.* **14**, 1020–1025 (2015).
15. Z. Liu *et al.*, *Phys. Rev. Lett.* **107**, 136805 (2011).
16. M. Wada, S. Murakami, F. Freimuth, G. Bihlmayer, *Phys. Rev. B* **83**, 121310 (2011).
17. S. Murakami, *Phys. Rev. Lett.* **97**, 236805 (2006).
18. M. Zhou *et al.*, *Proc. Natl. Acad. Sci. U.S.A.* **111**, 14378–14381 (2014).
19. C.-H. Hsu *et al.*, *New J. Phys.* **17**, 025005 (2015).
20. T. Kuzumaki *et al.*, *Surf. Sci.* **604**, 1044–1048 (2010).
21. R. H. Miwa, T. M. Schmidt, G. P. Srivastava, *J. Phys. Condens. Matter* **15**, 2441–2447 (2003).
22. See supplementary materials.
23. Y. Yao, F. Ye, X.-L. Qi, S.-C. Zhang, Z. Fang, *Phys. Rev. B* **75**, 041401 (2007).
24. G.-F. Zhang, Y. Li, C. Wu, *Phys. Rev. B* **90**, 075114 (2014).
25. D. Xiao, G.-B. Liu, W. Feng, X. Xu, W. Yao, *Phys. Rev. Lett.* **108**, 196802 (2012).
26. C.-C. Liu *et al.*, *Phys. Rev. B* **90**, 085431 (2014).
27. E. Mariani, L. I. Glazman, A. Kamenev, F. von Oppen, *Phys. Rev. B* **76**, 165402 (2007).
28. J. Voit, *Rep. Prog. Phys.* **58**, 977–1116 (1995).
29. A. Takayama, T. Sato, S. Souma, T. Oguchi, T. Takahashi, *Phys. Rev. Lett.* **114**, 066402 (2015).
30. C. Sabater *et al.*, *Phys. Rev. Lett.* **110**, 176802 (2013).
31. I. K. Drozdov *et al.*, *Nat. Phys.* **10**, 664–669 (2014).
32. F. Yang *et al.*, *Phys. Rev. Lett.* **109**, 016801 (2012).

ACKNOWLEDGMENTS

This work was supported by the Deutsche Forschungsgemeinschaft (DFG) through the Collaborative Research Center SFB 1170 "ToCoTronics" in Würzburg, the SPP 1666 Priority Program "Topological Insulators," and grant SCHA1510/5, as well as by the European Research Council (ERC) through starting grant ERC-StG-Thomale-336012 "Topolectrics." G.L. acknowledges the computing time granted at the Leibniz Supercomputing Centre (LRZ) in Munich. F.R. acknowledges many helpful discussions with M. R. Scholz and J. Aulbach. The authors declare no competing financial interests.

SUPPLEMENTARY MATERIALS

www.sciencemag.org/content/357/6348/287/suppl/DC1
Materials and Methods
Supplementary Text
Figs. S1 to S10
References (*33*–*44*)

15 August 2016; resubmitted 16 December 2016
Accepted 9 June 2017
Published online 29 June 2017
10.1126/science.aai8142

Science

Bismuthene on a SiC substrate: A candidate for a high-temperature quantum spin Hall material

F. Reis, G. Li, L. Dudy, M. Bauernfeind, S. Glass, W. Hanke, R. Thomale, J. Schäfer and R. Claessen

Science **357** (6348), 287-290.
DOI: 10.1126/science.aai8142originally published online June 29, 2017

Making a large-gap topological insulator

Although of interest to basic research, topological insulators (TIs) have not yet lived up to their technological potential. This is partly because their protected surface-edge state usually lives within a narrow energy gap, with its exotic transport properties overwhelmed by the ordinary bulk material. Reis *et al.* show that a judicious choice of materials can make the gap wide enough for the topological properties to be apparent at room temperature. Numerical calculations indicate that a monolayer of Bismuth grown on SiC(0001) is a two-dimensional TI with a large energy gap. The researchers fabricated such a heterostructure and characterized it using scanning tunneling spectroscopy. The size of the experimentally measured gap was consistent with the calculations.

Science, this issue p. 287